TREND

Supramolecular Chemistry

Macromolecular
Chemistry and Physics
www.mcp-journal.de

The Deconstruction of Supramolecular Structures Based on Modular Precise Macromolecules

*Chih-Hao Hsu and Stephen Z. D. Cheng**

To rationally design materials with desired properties, a modular approach based on volume- and shape-persistent nanobuilding blocks has been demonstrated recently. Constructing hierarchical supramolecular structures which span several length and energy scales is crucial to transfer and amplify the functionality of nanobuilding blocks to the bulk materials. Determination of soft material self-assembled structures thus plays a critical role in this approach; however, it is routinely the most time-consuming step due to the case-dependent sample preparation and insufficient number of X-ray and electron diffractions for direct structure determination. A rational thinking pathway for supramolecular structure determination is proposed in this article with covering a variety of essential concepts for a systematic case study. The scope of this article aims to guide newcomers in this field and expedite the molecular design screening for establishing a concrete relationship between molecular design and material properties—a part of the materials genome initiative.

1. Introduction

On the active search for advanced materials with tailored properties and functions, reliable methodologies to screen and evaluate materials based on the underlying structures, properties, processing, and performance are by now an established branch of materials research.[1] Most of the methodologies emphasize the characteristics of the fundamental components of a system and try to understand how these components eventually give rise to the functionalized macroscopic properties at the system level. However, to understand a complex content at the system level, such as in biology, solely investigating the isolated and specific components is far from sufficient. Instead, the interactions, structures, and interfaces among various length-scaled components in a system need to be taken into consideration.[2]

Hierarchical structures of functional entities in different length and energy scales have been recognized as critical to develop materials with desired properties. For example, ordered structures span in different length and energy scales, such as structures in structures, are capable of preserving the molecular functions and anisotropically transport/amplify to the material properties. Constructing a hierarchical structure can usually be achieved by self-assembly of individual components in a system, e.g., bottom-up approach. The challenge of a successful material development thus relies on the molecular design guided by the understanding of mutual effects and interactions among the components, such as enthalpic interactions and conformational entropy change, upon the hierarchical structure formation.

The thinking pathway of a rational and modular approach for molecular design in soft matter engineering has been proposed previously as the retro-functional analysis (RFA).[3,4] RFA starts from the desired material properties, and the required molecular function and hierarchical structure associate with the specific material property are linked to the functional synthon and structural synthon, respectively, of the molecular design (**Figure 1**). Structural synthons are entities to provide the scaffold of constructing hierarchical structures. Because of the need of spanning several different length scales, structural synthons encompass various noncovalent interactions in sub-nanometer scale, molecules with specific shapes in nanometer scale, and self-assembled structures from couple nanometer to micrometers. A functional synthon can be simply a chemical functional group, a certain arrangement of functional groups, a designed chemical sequence, or it can be an individual molecule, or even more complexed as a supermolecule and supramolecular assembly. No matter the complexity is, a functional synthon holds the underlying functionality of the material. The merit of RFA lies on the self-refinement process: each new molecular design is refined by the feedback of previous cycles of study. Consequently, the success of RFA highly relies on a high-throughput screening due to the "self-evolution" nature and thus, a large amount of prior information experiencedly corrected. The recent emerge "click chemistry" and other efficient organic transformations facilitate reliable synthetic routes for constructing precise and modular target molecules.[5–8] With the well adaption of these chemical tools, the synthesis of novel molecules based on molecular building blocks can be achieved with no hassle. Apart from the precise synthesis, the route from molecular design to hierarchical structure is usually the rate determine step of the whole

---

Dr. C.-H. Hsu
The Molecular Foundry
Lawrence Berkeley National Laboratory
Berkeley, CA 94720, USA
Prof. S. Z. D. Cheng
Department of Polymer Science
College of Polymer Science and Polymer Engineering
The University of Akron
Akron, OH 44325, USA
E-mail: scheng@uakron.edu

DOI: 10.1002/macp.201700390

process due to the highly case-dependent sample preparation and structural determination. For most of soft materials, growing sufficiently large single crystals (several micrometers in size) are extremely challenging. Also, supramolecular structures may not possess long-range order of atomic position but only certain orientational or positional order of motifs. These features of supramolecular soft materials limit themselves from generating sufficient amount of diffractions (>1000), and thus the structure cannot be straightforwardly determined by the single crystal X-ray diffractometer.

Since there is no single master-method to determine supramolecular structures, a systematic summary of representative cases should be able to highlight the common concepts in determine supramolecular structure and guide newcomers in this field to overcome the barrier of solving structure of new materials for the first time. In this article, we aim to leverage the extensive works on supramolecules in our group to develop a rational thinking pathway (pattern) of resolving the molecular packing and crystal structure in different length scales on the basis of building blocks.

2. Insights of Structure Determination for Giant Molecules

Investigating the outcome at the material level by manipulating the arrangement of atoms as we want has fascinated material scientist for decades.[9] Up until recently, arbitrarily controlling atom positions in a material remains as an unreached goal. To be in line with and stay as close as possible to the ultimate goal in material design, we aim to manipulate the position of a cluster of atoms instead of individual atoms. The cluster of atoms was coined as "nanoatoms," which are the primary building blocks for the supramolecular system we will cover in this article. "Nanoatoms" are usually, but not limits to, cage-like molecules, where the relative positions of individual atoms are preserved during supramolecular structure formation due to the volume- and shape-persistency of these "nanoatoms." "Nanoatoms" possess target molecular functions and/or the ability to form target structural scaffold driven by crystallization or the surface functionality. The most common "nanoatoms" and the ones will be covered in this article are [60]fullerene (C_{60}),[10–12] polyhedral oligomeric silsesquioxane (POSS),[13–16] and polyoxometalate (POM)[17–22] (**Figure 2**). This concept is similar to the "artificial atoms" in describing quantum dots,[23] metal nanoparticles,[24,25] and the "nanoscale atoms" for pseudo-spherical molecular clusters.[26] These "nanoatoms" can be combined with or without other building blocks, such as dendrimers,[27] polymers,[28,29] liquid crystals,[30,31] and others, to form a new class of self-assembling soft materials—giant molecules. Giant molecules are size-amplified small-molecules analogues with precisely defined composition, sequence, and geometry. Like other soft materials with chemically distinct building components, i.e., surfactants, thermotropic liquid crystals, and block copolymers, the self-assembly is governed by the driving force of filling space with an essentially uniform density.[32] The modular approach to construct precise macromolecules based on functionalized "nanoatoms" facilitates the attribution the role of each component for the final material property and expedite the study of RFA process.

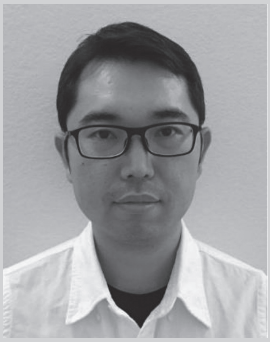

Chih-Hao Hsu currently works as a postdoc in the Molecular Foundry at the Lawrence Berkeley National Laboratory with Dr. Jeff Urban. He received his bachelor of science degree in chemical engineering at National Taiwan University in 2005, master of science degree in applied chemistry at National Chiao Tung University in 2007, and PhD degree in polymer science at the University of Akron in 2014 under the supervision of Prof. Stephen Cheng. His research interests focus on constructing and determining ordered supramolecular structures based on nanometer-sized motifs and utilizing phase-change materials for water desalination processes.

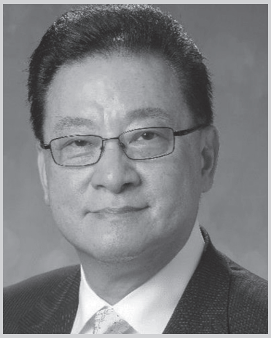

Stephen Z. D. Cheng is the Frank C. Sullivan Distinguished Research Professor, the R. C. Musson and Trustees Professor at the University of Akron. He received his PhD degree in chemistry at Rensselaer Polytechnic Institute in 1985. His research interests include ordered structure, morphology, phase transition thermodynamics, kinetics, and molecular motions in polymers and other soft materials.

The process of supramolecular structure determination is consisted of four steps: thermal analysis, phase determination, lattice characterization, and motif packing determination. The experimental techniques associated with each step have been summarized in Figure 1. Thermal analysis firstly helps us to understand the thermodynamic phase behavior and kinetics of phase transitions. It requires specifically careful that most of the phase behavior are not at thermodynamic equilibrium, rather in metastable states. The following phase determination focuses on the morphology of the phase we interested. The information of lattice and the associated space group will then be extracted utilizing small-angle X-ray scattering (SAXS), wide-angle X-ray diffraction (WAXD), and electron diffraction (ED) techniques. Finally, the packing scheme of motifs in a lattice can be realized via computer simulation based on experimental diffraction patterns and measured densities. The motif is the smallest unit to be considered as a whole in the supramolecular structure. In the system of giant molecules, motifs can be a single atom, a group of atoms, a "nanoatom," or even a whole molecule depends on the complexity and geometry of the

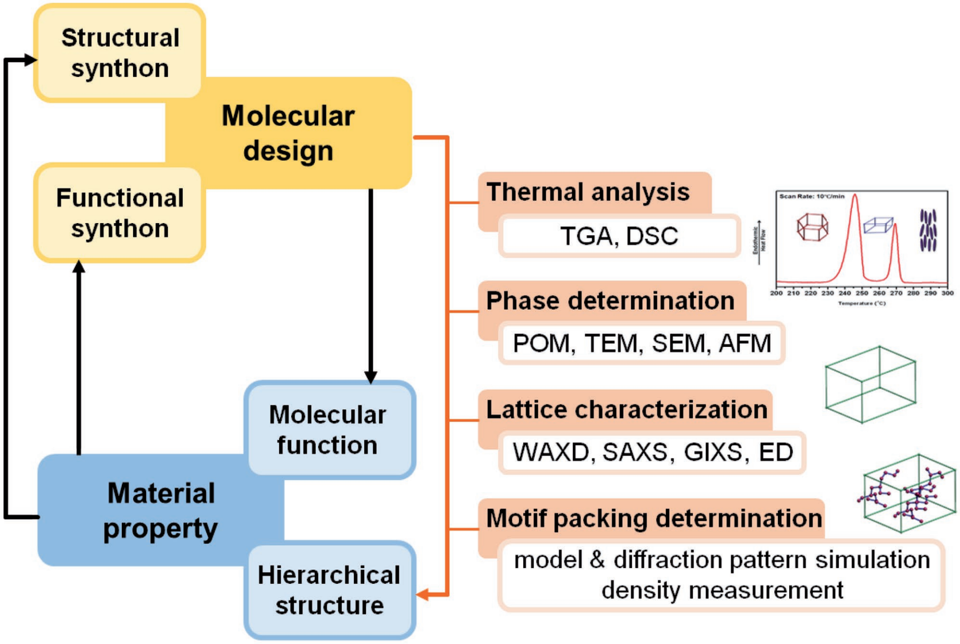

Figure 1. Relationship of RFA and controlled-assembly determination. The techniques for structure determination include thermogravimetric analysis (TGA), differential scanning calorimetry (DSC), polarized optical microscopy (POM), transmission electron microscopy (TEM), scanning electron microscopy (SEM), atomic force microscopy (AFM), wide-angle X-ray diffraction (WAXD), small-angle X-ray scattering (SAXS), grazing-angle X-ray scattering (GIXS), electron diffraction (ED), density measurement, and computer simulation.

chemical structure. Explanatory cases regarding to the structure determination will be introduced in the following sections. The first case is elaborated explicitly to cover as more essential concepts as possible and other cases convey supplementary concepts in different situations.

2.1. Bulk-Assembly 2D Materials

The symmetry breaking of the molecular entities usually does not destruct the original pristine bulk structure completely. Instead, certain packing scheme can be reserved. With a moderate modification on crystalline "nanoatoms," the lowered molecular symmetry will guide the functionalized "nanoatoms" to adopt a new molecular packing. The result structures of "nanoatoms" keep the original packing in the lateral dimension where no surface modification was introduced, generating the in-plane supramolecular structure (**Figure 3**c,f). The structural evolution along the out-of-plane direction can be controlled by the symmetry breaking components, such as chain lengths, spatial size, charges, etc. Comparing the observed structural information of 2D materials (e.g., SAXS, WAXD, and ED patterns) with its own bulk structure could provide the insight of in-plane structures. For example, the giant molecule consisted of C_{60} exhibits the identical "nanoatom" in-plane packing, which can be observed by ED (Figure 3a,b).[10] To specifically describe the "nanoatom" domain, a sub-lattice is needed to differentiate it from the whole lattice (**Figure 4**a). The lattice represents the packing of whole giant molecules with tetragonal lattice parameters of *a*, *b*, and *c*, and Miller index of *(hkl)*; while

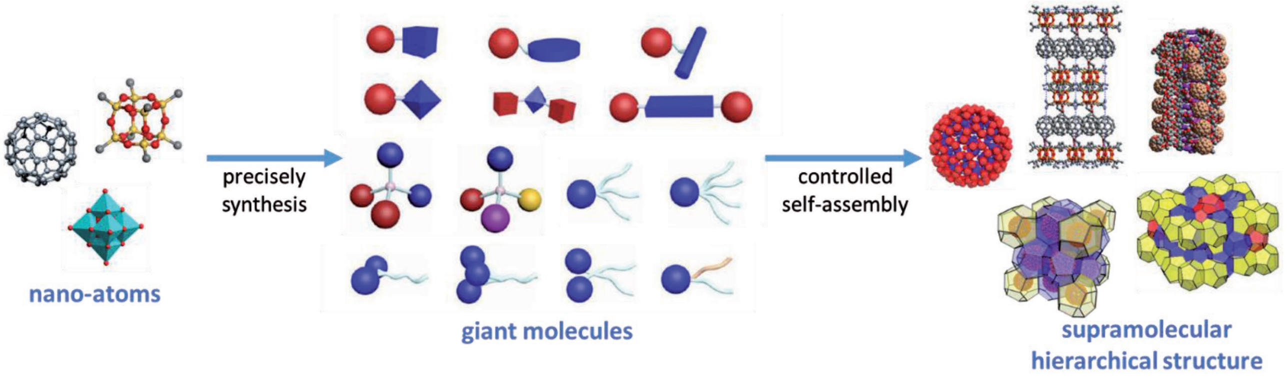

Figure 2. Illustration of building supramolecular hierarchical structures based on "nanoatoms" through giant molecules. Adapted with permission.[4] Copyright 2014, American Chemical Society.

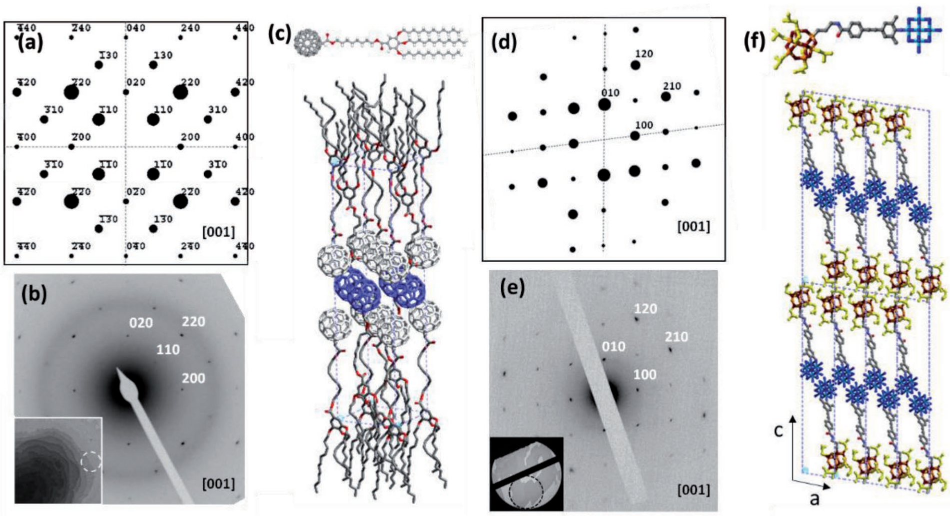

Figure 3. Comparison of bulk and 2D structure of C_{60}s and POSSs. Simulated ED pattern of triple layer of C_{60}s adapted from [001] zone of C_{60} bulk face-centered-cubic structure (a) and experimental observed ED pattern of 2D structure of C_{60}s (b) based on the triple-layered structural model (c). Simulated [001] zone ED pattern of BPOSS bulk structure[10] (d). Experimentally observed ED pattern of 2D structure of BPOSSs (e) based on the double-layered structural model (f). Reproduced with permission. Copyright 2014, WILEY-VCH Verlag GmbH & Co. KGaA, Weinheim. Copyright 2014, American Chemical Society. [17]

the sub-lattice only considers the packing of C_{60} in its domain. The corresponding tetragonal sub-lattice parameters are *a*, *b*, and *c′*, and Miller index of *(hkl′)*.

While comparing the WAXD patterns, the similarity of *(hk0)* diffractions, e.g., (*220*) and (*420*) diffractions in Figure 4c confirms the identical in-plane packings. The additional diffractions in the WAXD pattern represent the crystalline planes associated with the *c*-axis or the *c′*-axis. The first several diffractions have a relationship of integer multiples in *q* values, and this set of diffractions can be easily distinct from others in a fiber pattern (e.g., diffraction pattern of an orientated sample),[10,33,34] unambiguously suggesting a layered hierarchical structure.

The whole lattice can be determined by the above-mentioned information sufficiently; however, knowing the *c′*-axis of the sub-lattice requires further examinations. The information of the out-of-plane dimension of sub-lattice can be obtained by either operating the ED tiling experiment on flat-on samples or the regular ED experiment on edge-on samples. Flat-on samples can usually be achieved by drop-cast dilute solution (0.02 wt%) followed by thermal annealing.[10,11] On the other hand, edge-on samples can be achieved by soft epitaxial growth.[35,36] Because a successful soft epitaxy requires a lattice mismatch < 10% between samples and soft epitaxy agents (i.e., benzoic acid), finding a proper soft epitaxy agent is not guaranteed. Tiling ED pattern of flat-on samples is thus a more universal method to gain information of out-of-plane direction of a sub-lattice.

Upon rotating the flat-on sample along a certain axis, the corresponding reciprocal lattice is tilted simultaneously. With continuously sample tilting, different sets of *(hkl′)* diffractions

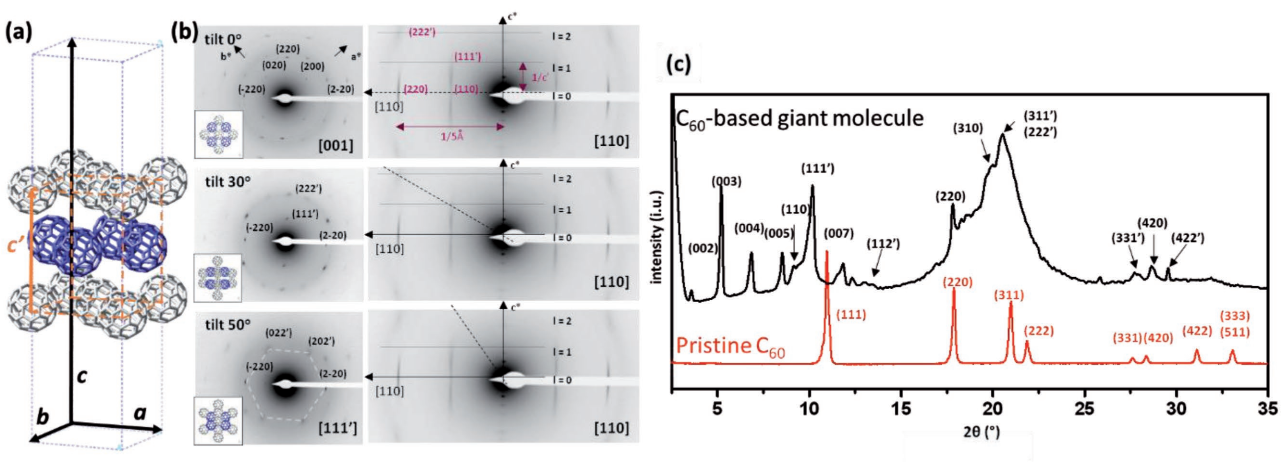

Figure 4. a) The illustration of the lattice and the corresponded sub-lattice of the C_{60}-based giant molecule. b) ED tilting experiments of the C_{60}-based giant molecule. c) Comparison of WAXD patterns between the C_{60}-based giant molecule and pristine C_{60} face-centered-cubic structure. Reproduced with permission.[10] Copyright 2014, WILEY-VCH Verlag GmbH & Co. KGaA, Weinheim.

intersect with the Ewald's sphere and reveal the out-of-plane information. The ED tiling on a C_{60}-based giant molecule is illustrated in Figure 4b as an example. As shown in Figure 3, the [001] zone ED pattern of the C_{60}-based giant molecule exhibit an identical [001] zone pattern as the pristine C_{60}s, which possess a face-centered cubic structure. Upon tilting 30° along its$^{[1-10]}$ direction (e.g., the long axis of the beam stop shown in Figure 4b), a new set of *(111′)* and *(222′)* diffractions emerged along the perpendicular direction of the beam stop. Finally, a set of pseudo-hexagonally arranged diffractions appeared at the tilt angle of 50°, indicating a [111′] zone of the supramolecular structure. The d-spacings of diffractions in a specific zone and the associated tilt angle allow us to calculate the length of out-of-plane axis. For the specific case of this C_{60}-based giant molecule, the tilting experiment confirms the packing of C_{60}s along the out-of-plane axis is sparser than in-plane packing (Figure 4a). In contrast to discrete diffraction spots in a perfect single crystal, the insufficient number of repeated lattices along the out-of-plane direction of a 2D material results in elongated diffraction rod in the reciprocal space ([110] zone ED patterns in Figure 4b), potentially limiting the accuracy of the correct tilting angle. The structural information of out-of-plane axis extracted from ED tilting should then be refined by matching the diffractions in both SAXS and WAXD patterns (Figure 4c).

The molecular packing and the associated lattice can then be visualized via computational packages, such as Accelrys Cerius.[2] The number of motif (*Z*) in the determined lattice is determined by the measured density. Finally, the molecular conformation and packing is determined by the energy minimization and the comparison between experimentally observed and simulated ED patterns qualitatively in peak positions and quantitatively in peak intensities.

2.2. Solution-Assembly 2D Materials

By sophistically design the surface functionalization of "nanoatoms," the structural growth along the lamellar normal direction can be prevented to fabricate 2D nanosheets (double-layered structure of giant molecules) via solution assembly. Unlike mechanical/chemical exfoliation of layered bulk materials such as clays, graphite, and boron nitrides, the approach to 2D nanosheets based on giant molecules is able to form single-layered nanosheets (double molecular thickness) with regular geometry and uniform lateral dimensions. Two categories of this type of self-assembly will be covered in this section: crystallization- and noncrystallization-driven processes.

The conjugate of a *t*-butyl-POSS with a Lindqvist-type POM (BPOSS-POM) is the representation of crystallization-driven case of 2D nanosheets, so called nanocrystals.[17] With a commensurate spatial size (≈1 nm in diameter) on both ends of the giant molecule, the strong tendency of crystallization for BPOSS provides the flat scaffold for the supramolecular nanocrystals. By using polar selective solvents of POMs (e.g., acetonitrile and dimethylformamide) for self-assembly, the surfaces of double-layered structure will be occupied by negatively charged POMs. The repulsive electrostatic interactions from both top and bottom surfaces of the nanosheet prevent aggregation of layers along the layer normal direction, resulting isolated nanocrystals (**Figure 5**b). The double-layered structure can first be confirmed by atomic force microscopy (AFM) measurement to show the

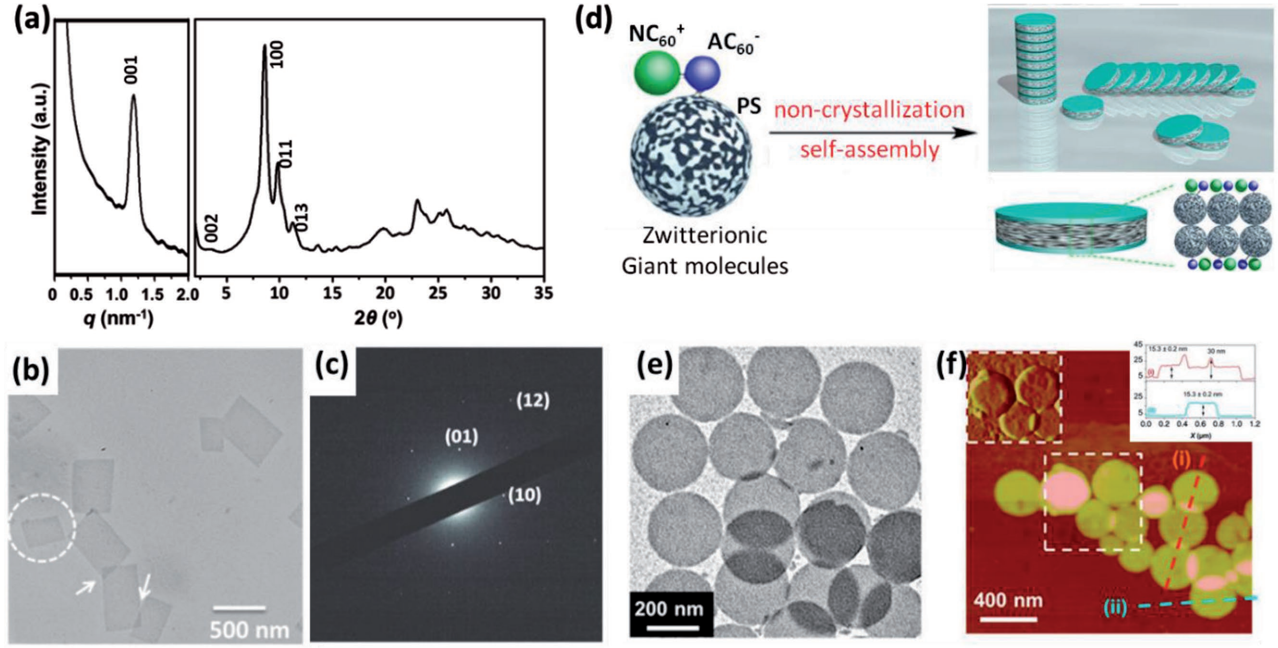

Figure 5. Crystallization- and noncrystallization-driven self-assembly in solution. a) SAXS and WAXD patterns of BPOSS-POM 3D structure. TEM image of 2D single crystal of BPOSS-POM b) and the corresponding ED pattern c). d) Illustration of noncrystallization-driven NC_{60}^{+}-AC_{60}^{-}-PS self-assembly. TEM (e) and AFM (f) images of the self-assembled 2D nanocoins based on the NC_{60}^{+}-AC_{60}^{-}-PS giant molecule. Reproduced with permission.[17,37] Copyright 2014 and 2017, American Chemical Society.

thickness of nanocrystals equal to two times of the length of BPOSS-POM. Further, the ED pattern of 2D nanocrystals shows a strikingly similarity to the 3D crystal structure of BPOSS-POM (grow from acetone solution, Figure 3d–f), indicating an identical in-plane packing. Determining the 3D crystal structure thus becomes the priority to understand the 2D nanocrystal structure.

The process of determining BPOSS-POM 3D structure is similar to the previous C_{60}-based case. First, comparing the ED patterns between BPOSS-POM and pristine BPOSS crystals to know which crystalline plane does the BPOSS cages in BPOSS-POM crystal follow. In this case, the double-layered packing of BPOSS cages arranged in the same way as the *ab*-plane of pristine BPOSS crystals. Diffractions with d-spacings around 1 nm are the most profound signals in the WAXD pattern (2θ = 8–10°) due to the interdistance between BPOSS cages (Figure 5a). Indexing part of the diffractions on WAXD pattern can then be made based on the known crystalline planes on ED patterns and the layered structure, *(00l)*. The rest observed diffractions can be further fitted by proposed lattice with considering all the known structural information.

On the other hand, a series of zwitterionic giant molecules contain both positively and negatively charged C_{60}s and a polystyrene (PS) tail (abbreviated as $NC_{60}{}^{+}$-$AC_{60}{}^{-}$-PS) represent the noncrystallization-driven case of 2D sheets (Figure 5d).[37] This particular giant molecule has been demonstrated to self-assembly into 2D circular nanostructures, so called nanocoins. The unique round-shape of 2D nanocoins is originated from the corresponding 3D lamellar cylindrical colloids. The 2D nanostructure is unstacked from the 3D cylindrical structure by changing pH value to ionize the C_{60}-based "nanoatoms." Due to the lack of crystalline structure, the study of molecular packing scheme relies on the effect of controlling factors on morphology change. The controlling factors include the length of PS tail and the degree of ionization of "nanoatoms." From the analysis of transmission electron microscopy (TEM) images of the 3D structure, a constant thickness of "nanoatom" domain (4.0 nm) was found with different PS chain length. It also shows a linear relationship between the radius of gyration (R_g) of PS chains and the thickness of PS domain, which is basically two layers of PS random coils stacked to each other. The TEM and AFM images (Figure 5e,f) of 2D nanocoins then further confirm a double-layered structure with PS domain sandwiched by charged "nanoatoms." Moreover, the connected positively and negatively charged "nanoatoms" are lying on the PS surface instead of stacking on each other based on the thickness of "nanoatom" domain and the fact that nanocoins can be separated (interdigitation of stacking conformation will hinder the layer separation).

3. From Conventional Self-Assembled Phases to Frank–Kasper Phases

The length scale of structures discussed above is centralized in nanometers, and the structural motifs ranged from "nanoatoms" to a single giant molecule. The associated structure determination is heavily depended on WAXD and ED patterns. With specific design on the molecular geometry, constructing supramolecular crystals with a group of giant molecules as a structural motif is feasible. For example, asymmetric giant molecules can self-assembly into spheroids in the molecular level and then packed into a variety of spherical packing, including Frank–Kasper (F–K) and quasicrystal phases. The phase separation in the molecular level is usually driven by the immiscibility between molecular components (i.e., hydrophilic and hydrophobic "nanoatoms"), and the interfacial curvature between immiscible nanodomains created by asymmetric giant molecules induces the formation of spheroidal motifs. In this scenario, the size of motif will be tens or even hundreds of nanometers, and the structure determination will rely on SAXS and TEM to retrieve information from both real and reciprocal spaces.

Conventional self-assembled phases of soft materials include lamellae, hexagonally packed cylinders (HEX), double gyroid, and body-centered-cubic spherical packing (BCC).[38,39] Beyond these conventional phases, a wide range of phases with topological close packing of spheres (e.g., F–K phases)[40,41] have been found emerged in between HEX and BCC phases.[42,43] F–K phases were originally found in metal alloys and clathrates and then discovered in certain soft materials, such as dendrimers,[44] block copolymers,[45] and liquid crystals;[46] while recently, giant molecules have been demonstrated as a new class of soft materials to self-assemble into this set of unconventional phases.[42,47] A15-phase and σ-phase are the two most often observed F–K phases, where A15-phase (space group $Pm\overline{3}n$) possesses the lowest interfacial area between spheroids and σ-phase (space group $P4_2/mnm$) is a periodic approximant of quasicrystals.[48,49]

Giant molecules with a tetrahedral core and four "nanoatoms" on the vertices (so called giant tetrahedra, **Figure 6**a–c)[47] and giant molecules with a "nanoatom" tethered by multiple PS tails (Figure 6d–i)[42] are representatives to self-assemble F–K phases and even dodecagonal quasicrystal (DQC) in addition to conventional phases. The measurements of differential scanning calorimetry (DSC) and temperature-resolved SAXS were first used to assess the phase stability and transitions of these materials. The X-ray diffraction pattern of each F–K and QDC phase has its characteristic fingerprints with specific ratio of q-value of diffractions (Figure 6b,d–f). A comparison of experimental and known patterns can thus narrow down the phase of interests. To unambiguously confirm the determined phase, TEM images of ultramicrotomed or thin film samples with deterministic tiling patterns are essential. A15-phase and σ-phase possess 4^4 and $3^2.4.3.4$ tilings, respectively, and the QDC phase observed in soft matter usually exhibits a random tailing consisted of $3^2.4.3.4$, $3^3.4^2$, 4^4, and 3^6 tailings (Figure 6c,g–i). The corresponding fast-Fourier-transform analysis on TEM images provides the information of symmetry (i.e., 12-fold symmetry of QDC phase).

By leveraging the experience on the RFA process, it is possible to explore more F–K phases, such as Laves phases and μ-phase, through rationally designed giant molecules. To resolve an unexplored sphere-packing soft material structure, the 27 physical known F–K phases should be the first priority to consider.[50] The experimental SAXS pattern and TEM images should be compared with calculated structure factor and simulated images (with proper particle size and electron scattering strength for "nanoatoms") based on metal alloy models.[51]

4. Conclusions

Structure determination is a critical step to close the loop in the RFA process. The basic structure-determining process for giant

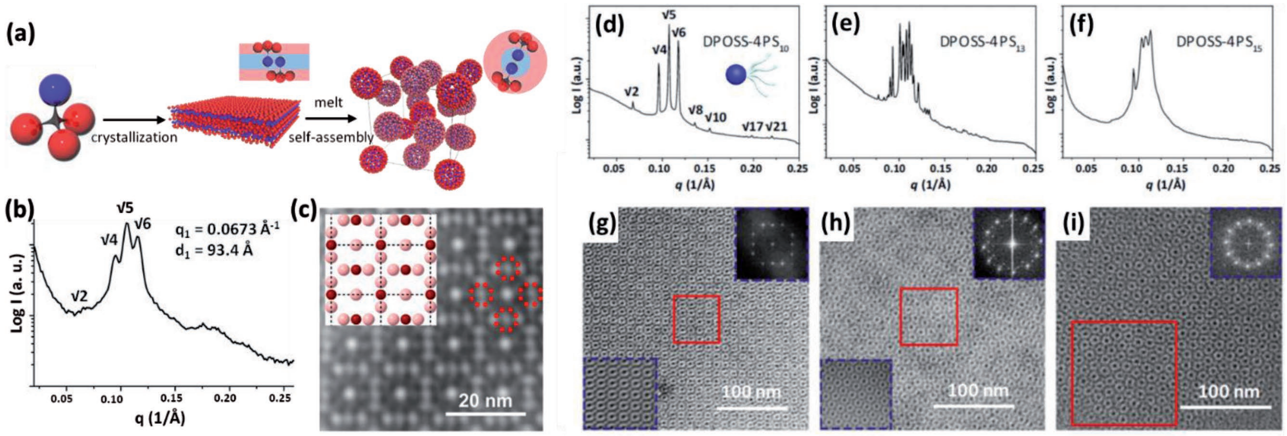

Figure 6. a) Schematic illustration of self-assembly for giant tetrahedron with three hydrophobic and one hydrophilic POSS cages. The SAXS pattern b) and TEM image c) of A15 phase constructed by the giant tetrahedron. The SAXS patterns (d–f) and the corresponding TEM images (g–i) of (hydrophilic POSS)-multiple PS chains, which represent the A15 (d,g), σ (e,h), and QDC (f,i) phases. Reproduced with permission.[47] Copyright 2015, American Association for the Advancement of Science.

molecules has been covered in the cases of self-assembled 2D materials in bulk and solution, crystallization- and noncrystallization-driven processes, and supramolecular F–K phases. The techniques can also applied to structured thin films with additional grazing incident X-ray scattering patterns.[52] On the foundation of current achievement on developing functional materials by rationally designed giant molecules, the prediction of supramolecular structures can be further improved by computational simulations. Despite the successful demonstration of Brownian dynamics simulation on giant molecules self-assembly into F–K phases,[42] developing a force field with considering “nanoatoms” as the basic entity for molecular dynamics simulation should be able to provide quantitatively predictions. This approach will require experimentally determined interaction parameters between “nanoatoms” and among all building blocks (both structural and functional synthons) used in the RFA process. We anticipate that rational thinking pathway of structure determination, combined with the RFA process, will lead to improvements in the molecular design of soft materials and structure–performance relationship developments.

Acknowledgements

This work was supported by National Science Foundation (DMR-1409972).

Conflict of Interest

The authors declare no conflict of interest.

Keywords

giant molecules, nanoatoms, self-assembly, supramolecular structures

Received: July 28, 2017
Revised: September 7, 2017
Published online:

[1] P. Yang, J.-M. Tarascon, *Nat. Mater.* **2012**, *11*, 560.
[2] H. Kitano, *Science* **2002**, *295*, 1662.
[3] W. B. Zhang, S. Z. D. Cheng, *Chin. J. Polym. Sci.* **2015**, *33*, 797.
[4] W.-B. Zhang, X. Yu, C.-L. Wang, H.-J. Sun, I. F. Hsieh, Y. Li, X.-H. Dong, K. Yue, R. Van Horn, S. Z. D. Cheng, *Macromolecules* **2014**, *47*, 1221.
[5] K. Yue, C. Liu, K. Guo, X. F. Yu, M. J. Huang, Y. W. Li, C. Wesdemiotis, S. Z. D. Cheng, W. B. Zhang, *Macromolecules* **2012**, *45*, 8126.
[6] K. Yue, C. Liu, K. Guo, K. Wu, X.-H. Dong, H. Liu, M. Huang, C. Wesdemiotis, S. Z. D. Cheng, W.-B. Zhang, *Polym. Chem.* **2013**, *4*, 1056.
[7] H. Su, J. K. Zheng, Z. Wang, F. Lin, X. Y. Feng, X. H. Dong, M. L. Becker, S. Z. D. Cheng, W. B. Zhang, Y. W. Li, *ACS Macro Lett.* **2013**, *2*, 645.
[8] Y. W. Li, X. H. Dong, K. Guo, Z. Wang, Z. R. Chen, C. Wesdemiotis, R. P. Quirk, W. B. Zhang, S. Z. D. Cheng, *ACS Macro Lett.* **2012**, *1*, 834.
[9] R. P. Feynman, *Eng. Sci.* **1960**, *23*, 22.
[10] X. Zhang, C.-H. Hsu, X. Ren, Y. Gu, B. Song, H.-J. Sun, S. Yang, E. Chen, Y. Tu, X. Li, X. Yang, Y. Li, X. Zhu, *Angew. Chem., Int. Ed.* **2015**, *54*, 114.
[11] T. Zhu, X. Zhang, Z. Li, C.-H. Hsu, W. Chen, T. Miyoshi, X. Li, X. Yang, Y. Tu, C. Li, *Chem. Commun.* **2017**, *53*, 8336.
[12] X. H. Dong, W. B. Zhang, Y. W. Li, M. J. Huang, S. O. Zhang, R. P. Quirk, S. Z. D. Cheng, *Polym. Chem.* **2012**, *3*, 124.
[13] X. H. Dong, R. Van Horn, Z. R. Chen, B. Ni, X. F. Yu, A. Wurm, C. Schick, B. Lotz, W. B. Zhang, S. Z. D. Cheng, *J. Phys. Chem. Lett.* **2013**, *4*, 2356.
[14] B. Ni, X.-H. Dong, Z. Chen, Z. Lin, Y. Li, M. Huang, Q. Fu, S. Z. D. Cheng, W.-B. Zhang, *Polym. Chem.* **2014**, *5*, 3588.
[15] X.-H. Dong, B. Ni, M. Huang, C.-H. Hsu, Z. Chen, Z. Lin, W.-B. Zhang, A.-C. Shi, S. Z. D. Cheng, *Macromolecules* **2015**, *48*, 7172.
[16] C.-B. Yu, L.-J. Ren, W. Wang, *Macromolecules* **2017**, *50*, 3273.
[17] H. Liu, C.-H. Hsu, Z. Lin, W. Shan, J. Wang, J. Jiang, M. Huang, B. Lotz, X. Yu, W.-B. Zhang, K. Yue, S. Z. D. Cheng, *J. Am. Chem. Soc.* **2014**, *136*, 10691.
[18] D. Li, P. C. Yin, T. B. Liu, *Dalton Trans.* **2012**, *41*, 2853.
[19] A. Proust, B. Matt, R. Villanneau, G. Guillemot, P. Gouzerh, G. Izzet, *Chem. Soc. Rev.* **2012**, *41*, 7605.
[20] M.-B. Hu, Z.-Y. Hou, W.-Q. Hao, Y. Xiao, W. Yu, C. Ma, L.-J. Ren, P. Zheng, W. Wang, *Langmuir* **2013**, *29*, 5714.

[21] C. Ma, H. Wu, Z.-H. Huang, R.-H. Guo, M.-B. Hu, C. Kübel, L.-T. Yan, W. Wang, *Angew. Chem.* **2015**, *127*, 15925.
[22] J. Tang, C. Ma, X.-Y. Li, L.-J. Ren, H. Wu, P. Zheng, W. Wang, *Macromolecules* **2015**, *48*, 2723.
[23] R. Bratschitsch, A. Leitenstorfer, *Nat. Mater.* **2006**, *5*, 855.
[24] M. A. Kastner, *Phys. Today* **1993**, *46*, 24.
[25] D. F. Perepichka, F. Rosei, *Angew. Chem., Int. Ed.* **2007**, *46*, 6006.
[26] X. Roy, C.-H. Lee, A. C. Crowther, C. L. Schenck, T. Besara, R. A. Lalancette, T. Siegrist, P. W. Stephens, L. E. Brus, P. Kim, M. L. Steigerwald, C. Nuckolls, *Science* **2013**, *341*, 157.
[27] X. H. Dong, X. C. Lu, B. Ni, Z. R. Chen, K. Yue, Y. W. Li, L. X. Rong, T. Koga, B. S. Hsiao, G. R. Newkome, A. C. Shi, W. B. Zhang, S. Z. D. Cheng, *Soft Matter* **2014**, *10*, 3200.
[28] Y. W. Li, Z. Wang, J. K. Zheng, H. Su, F. Lin, K. Guo, X. Y. Feng, C. Wesdemiotis, M. L. Becker, S. Z. D. Cheng, W. B. Zhang, *ACS Macro Lett.* **2013**, *2*, 1026.
[29] X. F. Yu, S. Zhong, X. P. Li, Y. F. Tu, S. G. Yang, R. M. Van Horn, C. Y. Ni, D. J. Pochan, R. P. Quirk, C. Wesdemiotis, W. B. Zhang, S. Z. D. Cheng, *J. Am. Chem. Soc.* **2010**, *132*, 16741.
[30] D.-Y. Kim, S. Kim, S.-A. Lee, Y.-E. Choi, W.-J. Yoon, S.-W. Kuo, C.-H. Hsu, M. Huang, S. H. Lee, K.-U. Jeong, *J. Phys. Chem. C* **2014**, *118*, 6300.
[31] Y.-J. Choi, D.-Y. Kim, M. Park, W.-J. Yoon, Y. Lee, J.-K. Hwang, Y.-W. Chiang, S.-W. Kuo, C.-H. Hsu, K.-U. Jeong, *ACS Appl. Mater. Interfaces* **2016**, *8*, 9490.
[32] C. M. Bates, F. S. Bates, *Macromolecules* **2017**, *50*, 3.
[33] H. Frey, S. Sheiko, M. Moller, J. C. Wittmann, B. Lotz, *Adv. Mater.* **1993**, *5*, 917.
[34] J. C. Wittmann, P. Smith, *Nature* **1991**, *352*, 414.
[35] C. De Rosa, C. Park, B. Lotz, J. C. Wittmann, L. J. Fetters, E. L. Thomas, *Macromolecules* **2000**, *33*, 4871.
[36] J. C. Wittmann, A. M. Hodge, B. Lotz, *J. Polym. Sci. Polym. Phys. Ed.* **1983**, *21*, 2495.
[37] Z. Lin, J. Sun, Y. Zhou, Y. Wang, H. Xu, X. Yang, H. Su, H. Cui, T. Aida, W. Zhang, S. Z. D. Cheng, *J. Am. Chem. Soc.* **2017**, *139*, 5883.
[38] M. W. Matsen, F. S. Bates, *J. Polym. Sci., Part B: Polym. Phys.* **1997**, *35*, 945.
[39] M. W. Matsen, F. S. Bates, *J. Chem. Phys.* **1997**, *106*, 2436.
[40] F. C. Frank, J. S. Kasper, *Acta Crystallogr.* **1959**, *12*, 483.
[41] F. C. Frank, J. S. Kasper, *Acta Crystallogr.* **1958**, *11*, 184.
[42] K. Yue, M. J. Huang, R. L. Marson, J. L. He, J. H. Huang, Z. Zhou, J. Wang, C. Liu, X. S. Yan, K. Wu, Z. H. Guo, H. Liu, W. Zhang, P. H. Ni, C. Wesdemiotis, W. B. Zhang, S. C. Glotzer, S. Z. D. Cheng, *Proc. Natl. Acad. Sci. USA* **2016**, *113*, 14195.
[43] S. Chanpuriya, K. Kim, J. Zhang, S. Lee, A. Arora, K. D. Dorfman, K. T. Delaney, G. H. Fredrickson, F. S. Bates, *ACS Nano* **2016**, *10*, 4961.
[44] X. B. Zeng, G. Ungar, Y. S. Liu, V. Percec, S. E. Dulcey, J. K. Hobbs, *Nature* **2004**, *428*, 157.
[45] S. Lee, M. J. Bluemle, F. S. Bates, *Science* **2010**, *330*, 349.
[46] G. Ungar, X. B. Zeng, *Soft Matter* **2005**, *1*, 95.
[47] M. Huang, C.-H. Hsu, J. Wang, S. Mei, X. Dong, Y. Li, M. Li, H. Liu, W. Zhang, T. Aida, W.-B. Zhang, K. Yue, S. Z. D. Cheng, *Science* **2015**, *348*, 424.
[48] S. Fischer, A. Exner, K. Zielske, J. Perlich, S. Deloudi, W. Steurer, P. Lindner, S. Förster, *Proc. Natl. Acad. Sci. USA* **2011**, *108*, 1810.
[49] T. M. Gillard, S. Lee, F. S. Bates, *Proc. Natl. Acad. Sci. USA* **2016**, *113*, 5167.
[50] M. D. Sikiric, O. Delgado-Friedrichs, M. Deza, *Acta Crystallogr., Sect. A: Found. Adv.* **2010**, *66*, 602.
[51] M. De Graef, M. E. McHenry, *Structure of Materials: An Introduction to Crystallography, Diffraction and Symmetry*, Cambridge University Press, Cambridge **2007**, p. xxxi.
[52] C.-H. Hsu, X.-H. Dong, Z. Lin, B. Ni, P. Lu, Z. Jiang, D. Tian, A.-C. Shi, E. L. Thomas, S. Z. D. Cheng, *ACS Nano* **2016**, *10*, 919.